Anomalous moisture sources of the Rhine basin during the extremely dry summers of 2003 and 2018

Imme Benedict [a,*], Chiel C. van Heerwaarden [a], Eveline C. van der Linden [b,f], Albrecht H. Weerts [c,d], Wilco Hazeleger [a,e]

[a] Meteorology and Air Quality Group, Wageningen University and Research, Wageningen, Netherlands
[b] Water Systems and Global Change Group, Wageningen University and Research, Wageningen, Netherlands
[c] Deltares, Delft, Netherlands
[d] Hydrology and Quantitative Water Management Group, Wageningen University and Research, Wageningen, Netherlands
[e] Faculty of Geosciences, Utrecht University, Utrecht, Netherlands
[f] Royal Netherlands Meteorological Institute (KNMI), Utrechtseweg 297, 3731 GA De Bilt, Netherlands

ABSTRACT

Droughts can be studied from an atmospheric perspective by analysing large-scale dynamics and thermody-namics, and from a hydrological perspective by analysing interaction of precipitation, evaporation, soil moisture and temperature at the land-surface. Here, we study it from both perspectives, and assess the moisture (evap-orative) sources of precipitation in the Rhine basin during the exceptionally dry summers of 2003 and 2018. We use ERA5 re-analysis data (1979–2018) and the Eulerian moisture tracking model WAM-2layers in order to determine the moisture sources of the Rhine basin. During an average summer, these evaporative sources are mostly located over the Atlantic Ocean, and there is a large contribution from continental evaporation, mostly from regions west of the Rhine basin. Both in 2003 and 2018 the absolute moisture source contribution declined over the ocean. In both years the anomalous moisture fluxes over the boundaries of the Rhine basin are mainly a result of anomalous wind and not because of anomalous moisture advection by the mean wind. Due to high pressure (blocking) over Europe, moisture is transported from the ocean with anticyclonic flow around the Rhine basin, but not into the basin. In 2018, unlike 2003, moisture is transported from the east towards the basin as a result of the anticyclonic flow around the Scandinavian blocking. The large-scale synoptic situation during the summer of 2018 was exceptional, and very favourable for dry conditions over the Rhine basin. Although blocking also occurred in 2003, the exact synoptic conditions were less favourable to dryness over the Rhine basin. In 2003 however, the recycling of moisture within the basin was much lower than the climatology and 2018, especially in August, possibly indicating the drying out of the soil resulting in the second heatwave in August 2003. To conclude, although the summer of 2003 and 2018 were both exceptionally dry, their characteristics in terms of moisture sources and recycling, and thereby their dependence on the large-scale circulation and land-atmosphere interactions, were found to be very different. It is therefore imperative that droughts are also studied as individual events to advance understanding of complex interactions between the large-scale atmospheric processes and the land surface.

1. Introduction

Drought is a multi-disciplinary problem with large societal and economic impact. Recent examples are the drought in 2003 in western Europe resulting in reduced crop yields, forest fires, overheated power plants, and most striking, excess death (Fischer et al., 2007; Schär and Jendritzky, 2004). During the dry summer of 2018 52% of the agricultural region over western Europe suffered from severe-to-extreme drought (Toreti et al., 2019).

The multidisciplinary aspect of drought is highlighted when explaining different drought perspectives. The climate perspective, to start with, focuses on synoptic situations such as atmospheric blocking conditions or other large-scale dynamic features (e.g. weather regimes, blocking indices, wave patterns), in relation to the climatology. The

meteorological view on drought is a lack of (or less-than-normal) precipitation, or a large imbalance between precipitation and evaporation. A hydrologist will describe drought as a lack of water in the soil-vegetation system, or as low river discharge. Lastly, drought from an ecological and agricultural perspective would focus on affected nature areas, forest fires, and reduced crop yields. These perspectives can be studied on a global scale, but are often also analysed for specific regions. The selection of these regions depends, again, on the different perspectives. A hydrologist probably focuses on a river catchment, where an ecologist would rather look to an area with similar vegetative conditions.

Here, we aim to combine the view of the climate/meteorologist and the hydrologist. We do so, by analysing the anomalous moisture sources, which are evaporative sources of precipitation over a region, of the Rhine river basin during the extremely dry summers of 2003 and 2018. We focus on the Rhine basin as hydrological catchment, which was clearly affected in 2003 and 2018, and where the lack-of-precipitation can also be translated to river runoff. By determining moisture sources of a basin, both large-scale dynamic and thermodynamic effects are captured, as well as land-atmosphere interactions, which gives further insights on the two drought events. In addition, evaporative sources, either continental (local) or oceanic (non-local) can give an indication of the vulnerability of the Rhine basin to ongoing and future land-use changes.

Moisture sources in relation to drought events are often studied for the US (Bosilovich and Schubert, 2001; Brubaker et al., 2001; Dirmeyer and Brubaker, 1999; Dominguez et al., 2006; Herrera-Estrada et al., 2019; Roy et al., 2018; Zangvil et al., 2004, 2001), while only few studies focus on central western Europe (Bisselink and Dolman, 2009; Rosner et al., 2019; Stojanovic et al., 2018), and none specifically for the Rhine catchment. On the other hand, the droughts of 2003, and to lesser extend 2018, are studied extensively in terms of large-scale circulation (Black et al., 2004; Black and Sutton, 2007; Cassou et al., 2005; Drouard et al., 2019; Kornhuber et al., 2019; Spensberger et al., 2020), land-atmosphere interactions (Ferranti and Viterbo, 2006; Fischer et al., 2007), hydrology (Philip et al., 2020) and future projections (Beniston, 2004; Schär et al., 2004; Stott et al., 2004; Vogel et al., 2019; Wehrli et al., 2020). Related to future projections, there is relatively high confidence and understanding in the thermodynamics aspects of drought under climate change (Shepherd, 2014), where increases in temperatures will result in more heatwaves and droughts in the future (Schär et al., 2004), as is also concluded specifically for the 2018 drought (Vogel et al., 2019; Wehrli et al., 2020). Differently, future changes in dynamics are very uncertain and not yet well understood (Shepherd, 2014; Woollings, 2010). For example, changes in frequency and persistence of blocking conditions are uncertain, especially because western Europe has a low signal-to-noise ratio (Woollings, 2010), and simulating blocking with high-resolution models remains challenging (Schiemann et al., 2016). Furthermore, soil moisture temperature and soil moisture precipitation feedbacks are shown to be important in droughts (Seneviratne et al., 2010), however the suggestion that droughts intensify and propagate via land-atmosphere feedbacks is not yet well understood (Miralles et al., 2019). To summarize, multiple aspects of droughts need further investigation, starting with understanding and simulating the current climate before projecting it towards the future. Here we take the approach by comparing two individual recent extreme drought events in terms of moisture sources, whereby we can combine the perspectives from the larger-scale circulation and the land-atmosphere interactions. With this perspective on moisture transport and recycling in light of the 2003 and 2018 drought, we bridge between the meteorological and hydrological communities. In addition, an event-approach is consistent with developing physical storyline approaches (Hazeleger et al., 2015; Shepherd, 2016), where understanding is advanced by studying complex physical, and potentially socio-economic and ecological interactions of individual climatological relevant events.

The objectives of this study are to (I) characterize and compare the 2003 and 2018 summer droughts in the Rhine basin in terms of moisture sources, (II) explain the differences and similarities in patterns of the moisture sources by analysing anomalies in wind and specific humidity separately and (III) put the dry summers further in context, by studying the inter-annual variability of summer precipitation over the Rhine in relation to large-scale circulation (blocking) and moisture recycling within the basin.

2. Methodology

2.1. ERA5 data

We use the latest reanalysis dataset ERA5 data (Hersbach et al., 2020) from the European Centre for Medium Range Weather Forecast (ECMWF). The spatial resolution of the ERA5 data is 0.25°. We obtain specific humidity and zonal and meridional wind at multiple levels in the atmosphere (850, 700, 500, 300, 200 hPa; Table 1). Further, we obtain zonal and meridional wind, precipitation, evaporation, surface pressure, and dewpoint temperature at or near the surface (Table 1). The wind and specific humidity variables provide instantaneous values. We use dewpoint temperature and surface pressure to obtain specific humidity at the surface. Further characteristics of the obtained variables are given in Table 1. We obtain the variables from 1979 until 2018 (40 years) over the following domain: 10°–75° N, and −105° E to 30° W (Fig. 1).

2.2. Theory and tracking method WAM-2layers

To determine the moisture sources of the Rhine basin we use the Eulerian moisture tracking method Water Accounting Model on 2-layers (WAM-2layers; Van der Ent et al., 2010; Van der Ent et al., 2014). This model solves for every grid cell the water balance, which we define here as:

$$\frac{\partial S}{\partial t} + \frac{\partial F_x}{\partial x} + \frac{\partial F_y}{\partial y} = E - P, \tag{1}$$

where $S = \frac{1}{\rho_w g} \int_0^{p_s} q \, dp$, $F_x = \frac{1}{\rho_w g} \int_0^{p_s} (qu) \, dp$, $F_y = \frac{1}{\rho_w g} \int_0^{p_s} (qv) \, dp$, ρ_w is the density of water, g is the gravitational constant, p_s is the surface pressure, 0 indicates the pressure at the top of the atmosphere, and q, u and v are defined in Table 1.

The water balance model is adapted to perform either forward (from evaporation forward in time to precipitation) or backward (from precipitation backward in time to evaporation) tracking. We use backward tracking of precipitation in the Rhine basin to determine the moisture sources. WAM-2layers performs the tracking on two integrated layers in the atmosphere, hence the atmospheric information is integrated to two layers. The model assumes well-mixed layers, and the division of the two

Table 1
Obtained variables from ERA5, including the levels in the atmosphere, time step and unit.

| Variable	Level(s) in the atmosphere	Time step	Unit
Zonal (east-west) wind u	10m + 850, 700, 500, 300, 200 hPa	6-hourly	m s^{-1}
Meridional (north-south) wind v	10m + 850, 700, 500, 300, 200 hPa	6-hourly	m s^{-1}
Specific humidity q	850, 700, 500,300,200 hPa	6-hourly	kg kg^{-1}
Evaporation E	Surface	hourly	m
Precipitation P	Surface	hourly	m
Surface pressure p_s	Surface	6-hourly	Pa
Dewpoint temperature $d2m$	2m	6-hourly	K
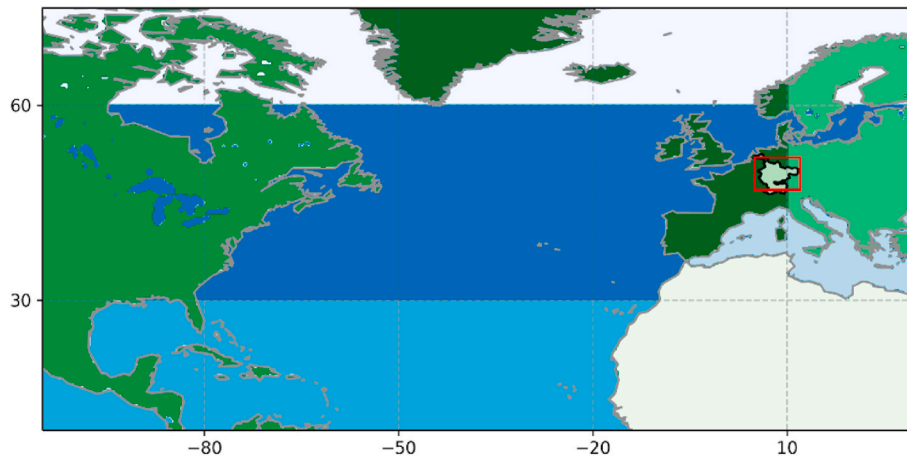
Fig. 1. Domain on which we perform the tracking, with the defined continental regions (North America, Africa, western Europe, Rhine basin, eastern Europe) and oceanic regions (tropical, extratropical, high latitudes, Mediterranean Sea) in different colours of respectively green and blue. We also indicated the Rhine basin and the box surrounding it is used to analyse the moisture fluxes over those boundaries. (For interpretation of the references to colour in this figure legend, the reader is referred to the Web version of this article.)

layers depends on the surface pressure by: $p_{divide} = 7438 + 0.72 * p_s$ [Pa] (van der Ent et al., 2013). Evaporation only contributes to the lowest layer, and transport between the layers occurs via vertical component F_v, which is determined from closing the water balance between the two layers. Last, to take into account the non-closure of the data, a sigma term is added, resulting in the following equation:

$$\frac{\partial S_{m,k}}{\partial t} + \frac{\partial F_{x,m,k}}{\partial x} + \frac{\partial F_{y,m,k}}{\partial y} = \delta P_k - E_{m,k} + F_v + \sigma_k, \qquad (2)$$

where m indicates tracked moisture, k indicates either the bottom or the top layers, and sigma indicates the source area of interest. In this study, $\delta = 1$ within and 0 outside of the Rhine basin. Note that E and P switched sign as backward tracking is performed. E_m are the resulting moisture sources that we will show throughout this study. For more information on the model we refer to Van der Ent (2014). This model was originally developed to perform moisture tracking with ERA-Interim reanalysis data, where the variables were saved at multiple model levels. Benedict et al. (2019) adapted WAM-2layers to perform tracking on climatic data at five pressure levels (850, 700, 500, 300 and 200 hPa), instead of multiple model levels (Benedict et al., 2019). For validation of this adapted version of WAM-2layers we refer to Benedict et al. (2019).

Here, we use this adapted version of WAM-2layers to determine the moisture sources of the Rhine basin with ERA5 data on five pressure levels. We tracked precipitation falling in the Rhine basin back in time during May-June-July-August. The model runs with a time step of 6 min, and the instantaneous moisture fluxes are linearly interpolated over time towards these 6 min time intervals. The model runs over the same domain as the variables were obtained: $10°–75°$ N, and $−105°$ E to $30°$ W.

In addition to analysing the moisture sources, another interesting variable to quantify is the amount of moisture recycled within a basin. The precipitation recycling ratio of a basin is the amount of precipitation occurring in a basin that is generated locally by evaporation (P_{local}), versus the total amount of precipitation occurring in a basin ($P = P_{local} + P_{advected}$). Thereby we assume that on monthly timescales almost all tracked evaporation within the basin results in local precipitation, the implications of these assumptions are in the discussion section. Hence the precipitation recycling ratio is defined as:

$$\rho_r = \frac{\int_A E_m dA}{\int_A P \, dA} \qquad (3)$$

where A is the area of the Rhine basin.

2.3. Experimental set-up

The analyses are focused on the Rhine basin, indicated in Fig. 1, and on the Northern Hemisphere summer period, here defined as May-June-July-August. We perform the analyses on a 40-year time period (1979–2018), with a focus on the summer of 2003 and 2018. Data is not detrended.

First, precipitation and discharge averages over May-June-July-August are analysed, to get a better overview of the anomalous events of 2003 and 2018 within the whole timeseries 1979–2018. We analyse monthly averaged daily observed discharge at Lobith (Rijkswaterstaat). In addition, we use temperature from ERA5 averaged over the Rhine basin to further elaborate on the events (not shown). Precipitation is obtained from the ERA5 re-analysis data, as will be used later for the moisture source analysis. We show the yearly cycle of daily precipitation and evaporation amounts, compared to the climatology. We apply a 20-day smoothed window on the daily timeseries, and we visualise one standard deviation around the climatological values.

Second, absolute moisture sources in mm month^{-1} are visualised spatially. We also show anomalies compared to climatology (summers 1979–2018) together with the anomalies of 500 hPa geopotential height obtained from ERA5. Normalized moisture sources (absolute moisture sources divided by the amount of precipitation occurring over the basin) are shown averaged over May-June-July-August and averaged over different regions. These regions are either continental or oceanic (Fig. 1): high latitude ocean (north of $60°$N), extratropical ocean (between $30°$ and $60°$N), tropical ocean (south of $30°$N), Mediterranean Sea, North America, Africa, western Europe (west of $10°$E) and eastern Europe (east of $10°$E).

Third, to further explore the results of the moisture sources, we take one step back and analyse the moisture fluxes (F_x and F_y) over the boundaries of the Rhine basin. We simplified the boundaries of the catchment with a box ($47°–52°$ N and $5°–12°$ W; Fig. 1), which makes the analyses on the moisture fluxes more straightforward and easier to interpret. For 2003 and 2018, we study the anomaly in moisture flux compared to the climatological flux per month, and whether this anomaly is a result of an anomaly in moisture (q') or in wind (u' or v'). With this analysis, we can further enhance our understanding which processes (dynamics or thermodynamics) played an important role during those anomalous events.

The zonal moisture flux F_x (uq) is studied over the eastern and western boundary of the box over the Rhine basin, and can be obtained as hourly values per month in 2003 and 2018:

$$uq = (u_c + u') * (q_c + q') = u_c q_c + u' q_c + u_c q' + u' q' \qquad (4)$$

where uq is the hourly flux in 2003 and 2018, u_c and q_c are the climatological monthly means, and u' and q' are the anomalies with respect to the climatological monthly mean. As we want to know the average flux over a boundary per month, we average over time (month), and over

latitude (47°–52° N) and height (900, 850, 700 and 500 hPa) along the boundary:

$$\langle uq \rangle = \langle (u_c + u^{'}) * (q_c + q^{'}) \rangle = \langle u_c q_c \rangle + \langle u^{'} q_c \rangle + \langle u_c q^{'} \rangle + \langle u^{'} q^{'} \rangle \qquad (5)$$

Rewriting gives:

$$\langle uq \rangle - \langle u_c q_c \rangle = \langle u^{'} q_c \rangle + \langle u_c q^{'} \rangle + \langle u^{'} q^{'} \rangle \qquad (6)$$

where the left hand side (LHS) indicates the total anomaly of a specific year and month over the boundary uq compared to the climatology $\langle u_c q_c \rangle$, and the right hand side (RHS) the contributions to the total anomaly from anomalies in wind $\langle u^{'} q_c \rangle$, moisture $\langle u_c q^{'} \rangle$, and combined wind and moisture $\langle u^{'} q^{'} \rangle$.

The same method is applied to separate the anomalies for the meridional moisture flux $F_y(vq)$ over the North-South boundaries, where we average over the same height (900, 850, 700 and 500 hPa) and over longitude (5° W to 12° W), resulting in:

$$\langle vq \rangle - \langle v_c q_c \rangle = \langle v^{'} q_c \rangle + \langle v_c q^{'} \rangle + \langle v^{'} q^{'} \rangle \qquad (7)$$

where the LHS indicates the total anomaly of a specific year and month over the boundary $\langle vq \rangle$ compared to the climatology $\langle v_c q_c \rangle$, and the RHS the contributions to the total anomaly from anomalies in wind $\langle v^{'} q_c \rangle$, moisture $\langle v_c q^{'} \rangle$, and combined wind and moisture $\langle v^{'} q^{'} \rangle$.

3. Quantifying the 2003 and 2018 summer droughts over the Rhine basin

Averaged over the Rhine basin, the summers of 2003 and 2018 have the lowest amount of precipitation of the last 40 years (Fig. 2). More precisely, the monthly average precipitation is 69.7 mm month^{-1} for 2003 and 68.8 mm month^{-1} for 2018, both deviating two standards from the mean (102 mm month^{-1}). By fitting a Gumbel distribution to the summer precipitation anomalies from 1979-2018, we find a return time of 20 and 40 years, for respectively the summer of 2003 and 2018. Also under averaging over June-July-August instead of May-June-July-August 2003 and 2018 are the driest summers in the time range. Thereby we have to note that the extremely dry year of 1976 is not included in this analysis as this ERA5 data is not yet available. We find an expected, positive correlation between precipitation over the Rhine basin and discharge at Lobith, with a correlation coefficient of 0.64. This correlation likely increases if evaporation is subtracted from precipitation, according to the hydrological water balance.
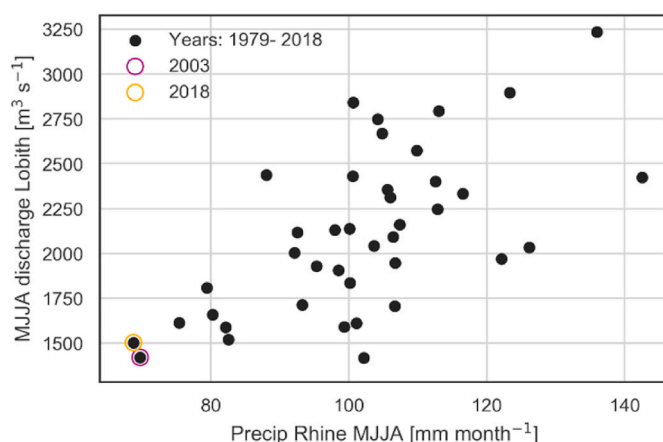

Fig. 2. May-June-July-August averages of precipitation over the Rhine basin in mm month^{-1} against May-June-July-August averages of discharge in Lobith in m^3 s^{-1} for every year from 1979 to 2018. The years 2003 and 2018 are indicated with respectively an orange and purple circle. (For interpretation of the references to colour in this figure legend, the reader is referred to the Web version of this article.)

The average discharge in Lobith over MJJA in 2018 (1 501 m^3 s^{-1}) and 2003 (1 419 m^3 s^{-1}) falls within the range of two standard deviations from the mean (2 103 m^3 s^{-1}). Lowest discharge averaged over four summer months occurred in 2011. In 2003 and 2018, high temperatures presumably also resulted in more snow melt from the Alps and therefore less exceptional values for discharge as we found for precipitation. However, later in the season exceptionally low discharges of 810 m^3 s^{-1} occurred in October–November 2018, compared to a climatology of 1809 m^3 s^{-1} in October–November. In this season, groundwater level and soil moisture content was probably still very low from the previous dry months, and snow melt does not play a role anymore. The year 2003 was not so exceptionally dry in October–November, however discharge was still on the low side (1 214 m^3 s^{-1}) compared to the mean.

3.1. Month-to month description of dry summer 2003

Fig. 3 shows the smoothed daily variations of precipitation and evaporation for the year 2003 and 2018, and also for the climatology. Although 2003 started in January with enormous discharge amounts reaching 9 500 m^3 s^{-1}, precipitation in the winter of 2003 was already below normal, except for the beginning of February (Fig. 3b). In March and April, daily precipitation values around 1 mm day^{-1} were found, while climatological values are around 2 mm day^{-1} (1 mm day^{-1} falls outside one standard deviation from the mean). During this period, a high-pressure system developed over western Europe, resulting in dry conditions. These dry conditions continued into May 2003, while the month ended rather wet. June shows the opposite signal, with a wet start and a dry ending of the month in terms of precipitation. Moreover, June was very warm with a positive temperature anomaly of 4.3 °C over the Rhine basin. Evaporation was much higher than average (more than one standard deviation) at the end of June, due to high temperatures, and possibly to increased radiation because of clear skies under the high-pressure system. In that period, probably enough water was present in the soils and plants to evaporate. Thereafter, daily evaporation values dropped below the climatology in July and even lower in August. The same signal is found for precipitation which is low in July, and even lower in August. Especially the middle-to-end of August was very dry. In addition, a second heatwave occurred in August 2003 affecting whole of southwestern Europe, with positive temperature anomalies of 4 °C over the Rhine basin.

3.2. Month-to-month description of dry summer 2018

The winter of 2018 started with daily precipitation rates above 5 mm day^{-1} (Fig. 3b), while end of February and beginning of March were rather dry. From May 2018 onwards high pressure over Scandinavia and western Europe resulted in fewer clouds, more incoming radiation and therefore higher evaporation rates. The latter is clearly visible from Fig. 3a with in May 2018 daily evaporation rates above one standard deviation from the climatology. Similarly, though opposite, less precipitation occurred from May onwards. The high-pressure system remained persistent until July, but disappeared shortly in June. During this blocking period, temperature was high and precipitation rates low. Precipitation rates were often more than one standard deviation less than the climatology, especially and consistently in July and August (Fig. 3). Evaporation over the Rhine basin was below climatology from July onwards. In contrast to 2003, where whole of Europe was dry, in 2018 north western Europe was dry while the south of Europe was relatively wet.

4. .Monthly moisture sources during the summer of 2018 and 2003 – comparison with climatology

The climatological moisture sources (averaged over 40 years) for the months May, June, July and August are shown in the left column of Fig. 4 and Fig. 5, and the integrated moisture fluxes derived from the
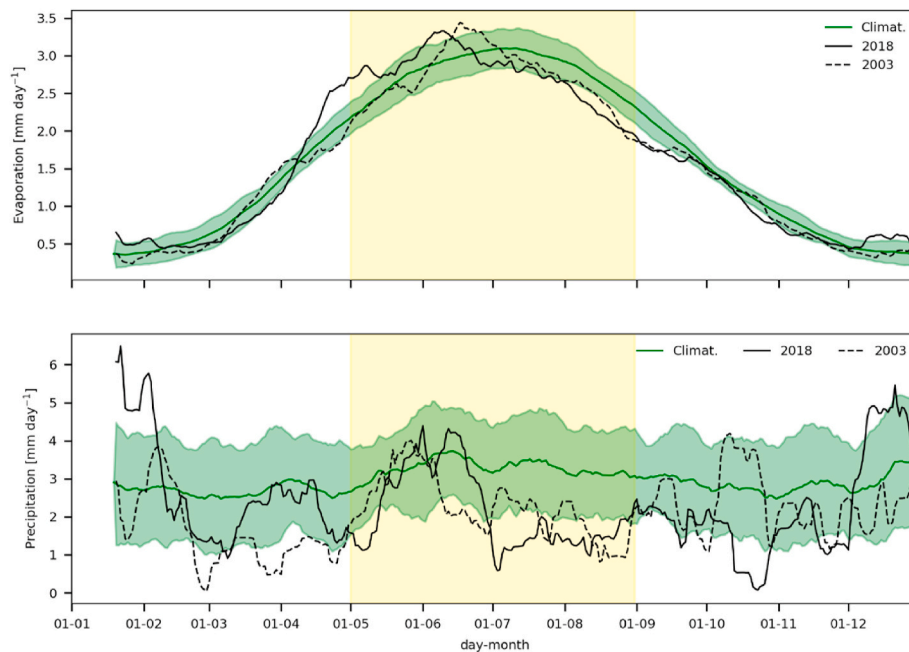
Fig. 3. (a) Evaporation and (b) Precipitation over the Rhine basin and over time in mm day^{-1} using a 20-day smoothed window, for the climatology (1979–2018) in green, and the year 2018 and 2003 in black straight and dotted respectively, all based on ERA5 reanalysis data. The green shading indicates one standard deviation of the 20-day smoothed window. (For interpretation of the references to colour in this figure legend, the reader is referred to the Web version of this article.)

tracking model WAM-2layers. The amount of precipitation over the Rhine basin is indicated in the subtitles. Fig. 6 shows the normalized moisture sources averaged per region (upper plot ocean region, and lower plot land regions). We first discuss the climatological moisture sources and fluxes, and then the sources specific for the two dry summers.

In all summer months the climatological moisture sources cover a large oceanic area, including the Caribbean Sea, Gulf of Mexico and the North Atlantic Ocean. Although the local contributions per grid cell appear small, a normalized average over the tropical and extra tropical North Atlantic (between 30° and 60° N) region results in about 50% of the precipitation in the Rhine basin (Fig. 6). Much smaller ocean contributions (~1–5%) come from the polar North Atlantic and Mediterranean Sea. Because of the pre-dominantly western winds, most (oceanic) moisture sources are located west of the Rhine basin. Over land, we find small contributions from North America, even smaller contributions from North Africa, and as expected larger contributions from west and eastern Europe, with increasing sources for decreasing distance to the basin. The largest moisture sources (~6 mm month^{-1}) are found in the Rhine basin itself, indicating high recycling of moisture over this region in summer. These large moisture sources over land happen because evaporation is highest in summer time over land (Fig. 3). The recycling of precipitation is around 8% in summer over the Rhine basin, and much lower in winter. When analysing the climatological moisture sources per summer month, only small differences between months appear, while the overall pattern is similar.

4.1. Description of the moisture sources in 2003 compared to climatology

2003 was the second driest summer over the Rhine basin in our 40-year time series, based on precipitation averages over May, June, July and August (see Fig. 2). Here, we discuss the moisture sources of the dry summer of 2003 (absolute sources in middle column and anomalies in right column Fig. 4) and in the next section for 2018, and thereafter we compare the sources for the two dry summers. The normalized sources per region are indicated in Fig. 6 for 2003 with an orange cross.

In May 2003 the precipitation over the Rhine basin is only 6 mm month^{-1} less than the climatology of about 100 mm month^{-1}. May 2003

is characterized by larger than normal moisture fluxes over the Atlantic Ocean, over the Netherlands and northern Germany towards the Baltic States. In this month, higher than normal pressure occurred over southern and eastern Europe and lower than normal pressure over Iceland (Fig. 4c), inducing stronger flow over the Netherlands (Black et al., 2004), as is also visible from the geopotential heights being closer together. The higher than normal pressure over the Iberian peninsula 'blocks' the moisture transport from those regions towards the Rhine basin, resulting in negative anomalies of absolute moisture sources from the Iberian peninsula.

In June 2003, there is a clear dipole in geopotential over the Atlantic and western Europe, with lower than normal pressure over the ocean and higher pressure over the continent, indicating an Atlantic Low weather regime (Cassou et al., 2005). The high pressure system over the Rhine basin induces a strong anti-cyclonic transport of moisture around/northward of the Rhine basin (Fig. 4e and f). As a result, only half of the precipitation compared to normal falls within the basin, 55.5 mm month^{-1} in 2003 whereas 102.4 mm month^{-1} precipitates in the climatology. Normalized, still more moisture came from western Europe and the Rhine basin itself (in this month primarily from Spain/southwest France), and there is also a small positive normalized contribution from the extratropical oceanic region (Fig. 6).

In July 2003 the high pressure system over western Europe weakens, but it is still present. The moisture fluxes are close to normal in this month, however the anomaly in absolute and normalized moisture source is negative over the entire ocean and land domain. There is also a negative anomaly in evaporation (1 mm day^{-1}, not shown) over the South of France, which indicates dry soils.

The pattern persists into August, with a negative anomaly in absolute moisture source over land, and half of the precipitation amounts (45 mm month^{-1}) compared to the climatology (97.3 mm month^{-1}). In this month we find lower moisture fluxes and the hypothesized dry soils could still persist. This is further discussed in Section 5.2 on the connection between recycling and precipitation within the basin.

4.2. Description of the moisture sources in 2018 compared to climatology

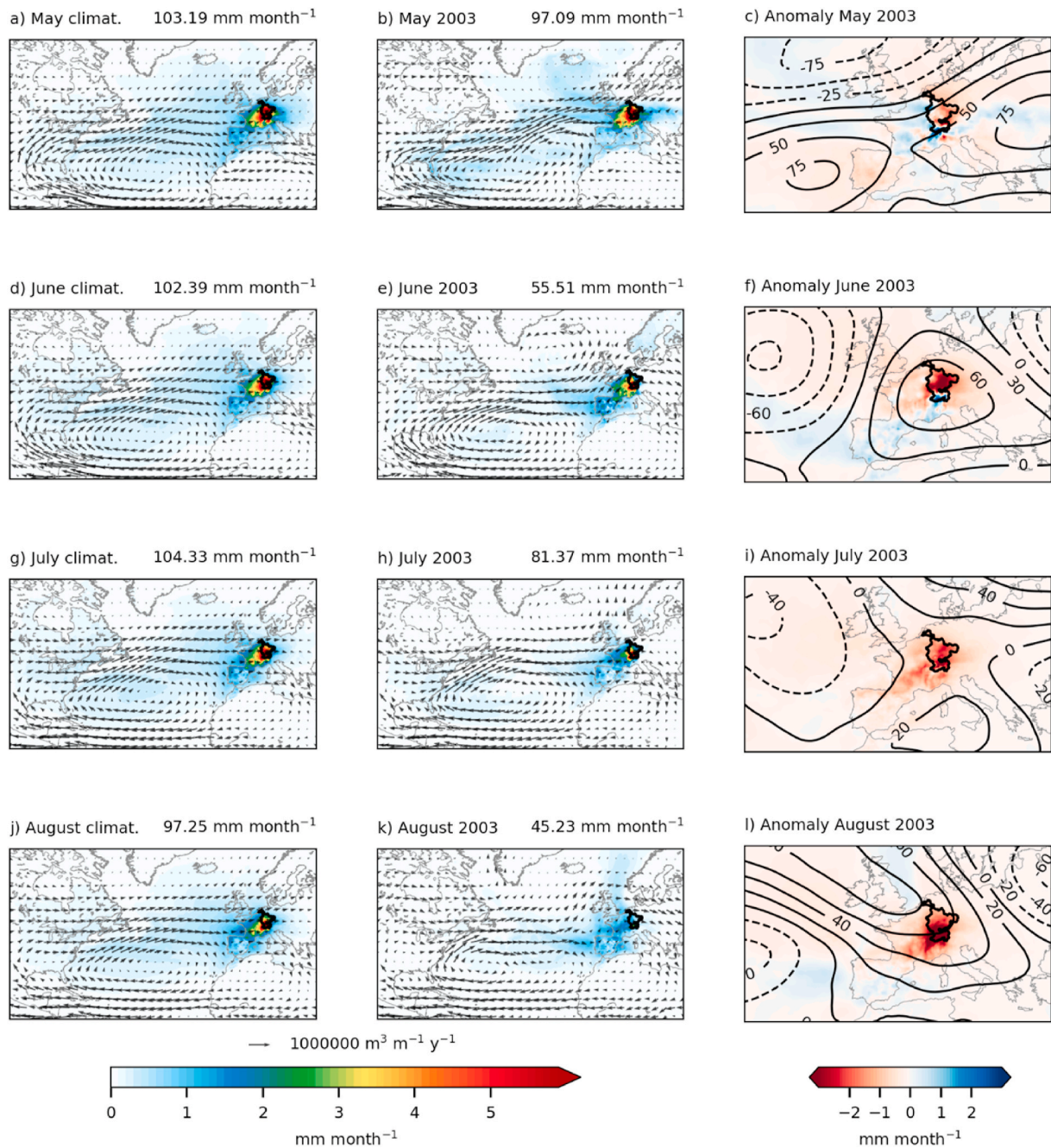In the second column of Fig. 5 we show the absolute moisture sources

Fig. 4. Absolute moisture sources (colours, mm month^{-1}) and vertically integrated moisture fluxes for May June July and August for the climatology (1979–2018) (a,d,g,j), and 2003 (b,e,h,k). The anomalous moisture sources are zoomed on the Rhine basin and the 500 hPa geopotential height anomalies (m) are also shown (c,f,i, l). Titles show the average precipitation over the Rhine basin in mm month^{-1}. (For interpretation of the references to colour in this figure legend, the reader is referred to the Web version of this article.)
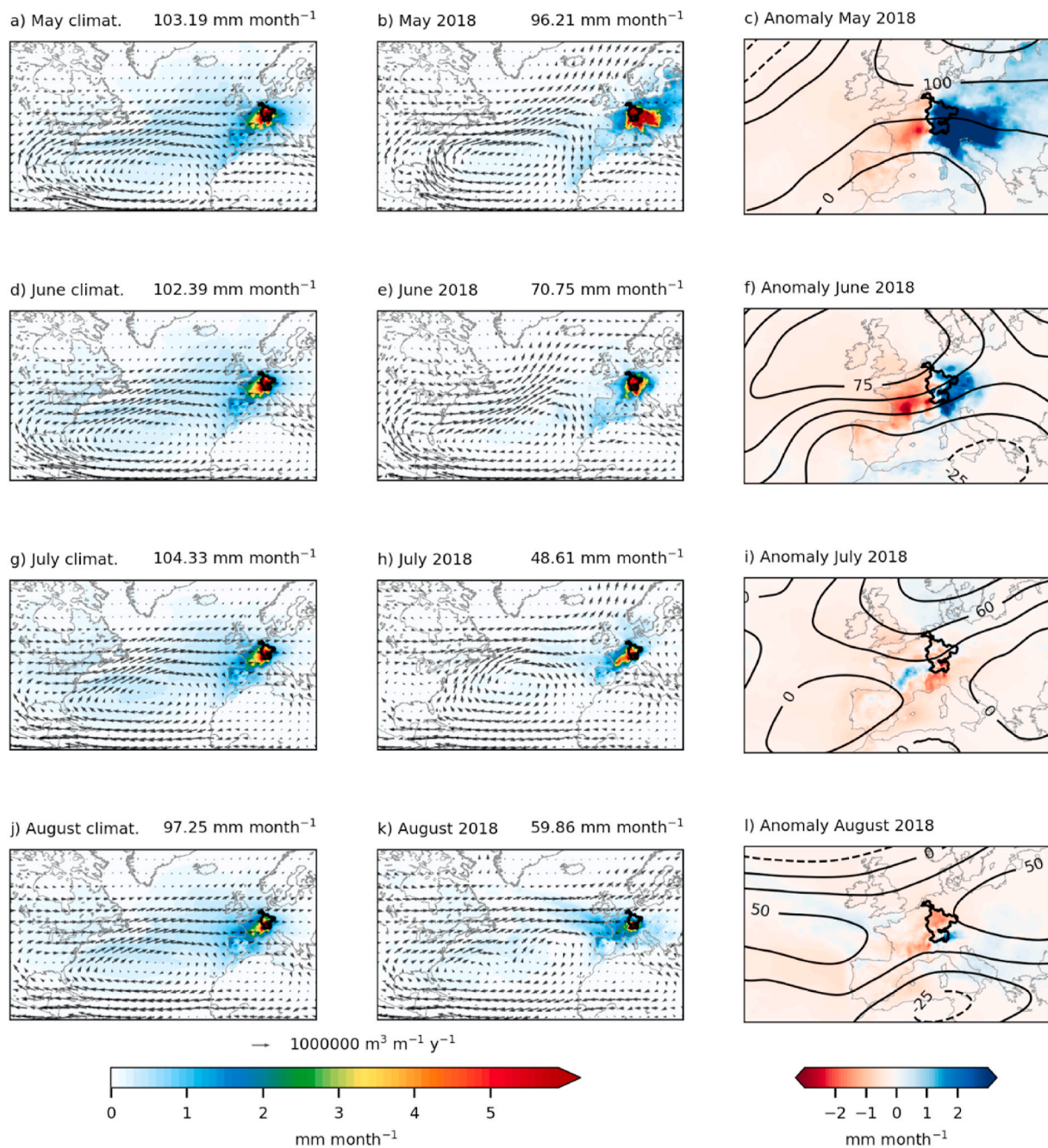
Fig. 5. Absolute moisture sources (colours, mm month^{-1}) and vertically integrated moisture fluxes for May June July and August for the climatology (1979–2018) (a,d,g,j), and 2018 (b,e,h,k). The anomalous moisture sources are zoomed on the Rhine basin and the 500 hPa geopotential height anomalies (m) are also shown (c,f,i, l). In the titles we indicate the average precipitation over the Rhine basin in mm month^{-1}. (For interpretation of the references to colour in this figure legend, the reader is referred to the Web version of this article.)

of May, June, July and August 2018, and in the third column the anomalies in absolute moisture sources, with a focus on the Rhine basin. In Fig. 6 the normalized moisture sources per region are indicated for 2018 with a purple cross.

In May 2018, we find much smaller moisture fluxes over the Netherlands, UK, France and Germany compared to climatology. Anomalous northward directed moisture fluxes are found along the coast of Scandinavia, and anomalous southward directed moisture fluxes at the coast of France and Spain. Hence, in May 2018, little moisture is transported from the west towards the Rhine basin, explaining the low amounts of moisture source contribution from the land region west of the Rhine basin, and from the Atlantic Ocean (Fig. 5b

and c). From the normalized moisture sources (Fig. 6), we find that the contribution from the extra tropical ocean region is almost half of its climatological contribution in May (18% in 2018 compared to 35% in climatology). In contrast, a large positive contribution in moisture source was found in May from eastern Europe, with a normalized contribution of 34% compared to the climatology where this amounts to 9%. This anomalous contribution of moisture source from eastern Europe is also clearly visible from Fig. 5b and c, and is explained by the moisture fluxes from east to west (to the Rhine basin) over Poland. This anomalous moisture transport in May 2018 is related to a high-pressure system which was located over southern Scandinavia, resulting in a blocking of the westward flow towards western Europe and an
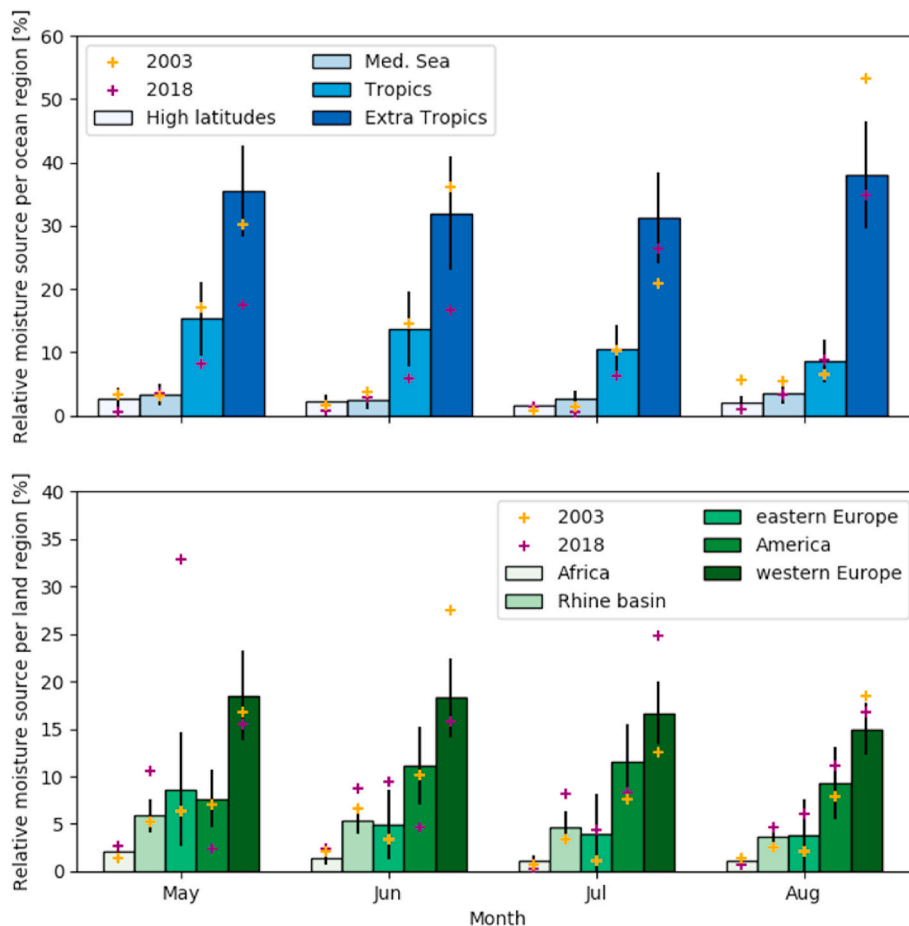
Fig. 6. Normalized moisture source contribution averaged over 40-years per ocean region (upper plot) and land region (lower plot) for the months May, June, July and August. The error bars indicate one standard deviation around the mean. Normalized moisture sources for 2003 and 2018 are indicated with orange and purple crosses. Regions are indicated in Fig. 1. (For interpretation of the references to colour in this figure legend, the reader is referred to the Web version of this article.)

enhancement of the anti-cyclonic flow from eastern Europe towards the Rhine.

In June 2018 the high-pressure system persisted and expanded over the United Kingdom and Ireland (Fig. 5f). The absolute moisture source anomalies show a similar pattern as in May 2018, with a negative anomaly west of the Rhine basin (Fig. 5f), which is in line with the small moisture fluxes west of the basin, and a positive anomaly east of the Rhine basin, although smaller than in May. The negative anomaly in terms of moisture sources from the extratropical ocean is also clearly visible from the normalized contributions (Fig. 6), where the contribution of June 2018 falls outside one standard deviation of the distribution. The normalized positive anomaly in moisture source contribution from eastern Europe falls outside one standard deviation as well, but is not as anomalous as in May. Together, the smaller contribution from the East, and the still negative anomaly from the Atlantic, leads to anomalously low precipitation in the Rhine in June 2018 ($\sim$70 mm month^{-1}) compared to the climatology (102 mm month^{-1}).

July was the driest month over the Rhine basin with precipitation amounts less than half of the climatological values ($\sim$48 mm month^{-1} in 2018 compared to 104 mm month^{-1} averaged over 40 years). The high-pressure anomaly persisted over Europe in July 2018, and expanded towards northern Scandinavia, resulting in strong northwards moisture fluxes over the North Sea and along the coast of Norway (Fig. 5h). The moisture fluxes over the Netherlands and the Rhine basin, and thereby the contribution of absolute moisture sources over the Atlantic, North America and West Europe, are still small, similar as for May and June

2018. The only exception is the mid-southern part of France, where the moisture sources are enhanced, as is clearly visible from Fig. 5i. In this dry month in July, we do find that the normalized sources over land are equal or higher than average, except for North America and Africa. Thus, in this exceptional dry month, there is relatively more moisture recycled locally over land. The relation between dryness and recycling is further investigated for all summers in the 40-year study period in Section 5.2. Besides, the large moisture fluxes found in the south of Europe in July 2018 likely explain the positive moisture source anomaly over the South of France, and can additionally explain the high precipitation amounts in southern Europe in July 2018 (Toreti et al., 2019), although that should be studied in more detail and is beyond the scope of this study.

In August 2018 the high-pressure anomaly (blocking) moved eastward into eastern Europe. As a result, moisture was transported further land inwards over western Europe compared to the previous months. Although more moisture could reach the Rhine basin, the absolute moisture sources are still anomalously low over the largest part of Europe and the Atlantic Ocean. However, the normalized moisture source contributions from land are higher compared to the average, except for Africa. Over land, negative anomalies in soil moisture, because of the preceding drought, could be an explanation of the low moisture sources. If we analyse evaporation from ERA5 for August 2018 compared to the climatology we find over western Europe negative anomalies of evaporation of 3 mm day^{-1} (Figure not shown), indicating dry soils.

4.3. Mechanisms of anomalous moisture fluxes – effects of wind and humidity

In the previous sections we found that during the drought of 2003 and 2018 moisture fluxes into the Rhine basin were anomalous, both in size and direction, resulting in anomalous moisture sources (Figs. 4–6). The moisture fluxes, and sources, give us a combined picture of changes in thermodynamics (i.e. moisture contribution to moist static energy) and changes in dynamics (wind speed and direction) during those extreme summers. Here, we will separate the contributions from anomalous moisture and anomalous wind, as described in the methodology, to quantify their contributions to the total moisture fluxes over the boundaries of the Rhine basin in 2003 and 2018. We first discuss the climatological fluxes and then the anomalies for 2003 and 2018, and which component contributed to these anomalies. The zonal moisture fluxes are indicated in Table 2, and the meridional moisture fluxes in Table 3 (LHS of Eq (6) and (7)). The total anomalies in 2003 and 2018, and the different anomalies contributing are shown in Figs. 7 and 8.

We find that in May, June, July and August the climatological zonal moisture fluxes increase over the course of summer from 8.55 to 6.34 kg kg^{-1} m s^{-1} in May to 22.25 and 18.78 kg kg^{-1} m s^{-1} in August, over the west and eastern boundary respectively. These zonal moisture fluxes increase over summer, as more moisture is available for transport due to higher temperatures and more evaporation. The climatological zonal moisture flux over the eastern boundary is always smaller than over the western boundary, as wind speeds decrease over land. The climatological meridional (north-south) moisture fluxes (Table 3), are much smaller than the zonal moisture fluxes (Table 2), as the flow is predominantly westerly. The largest meridional fluxes are found in May and August, and the meridional fluxes over the northern boundary are always larger than the fluxes over the southern boundary. The latter is related to lower windspeeds in the south, as moisture levels are higher in the south because of higher temperatures.

Contributions to anomalous moisture fluxes in 2003 In May 2003 we find a doubling of the zonal moisture flux, both over the western and eastern boundary (see also Fig. 4b). Nevertheless, there is still divergence of moisture within the marked region, as the flux over the north boundary is remarkably large as well (see next section). The anomalous

zonal moisture flux is a result of anomalous zonal wind (green bar Fig. 7a–b). This positive anomaly in zonal moisture flux is still present although much smaller in June, where the anomaly is a result of both anomaly in moisture and wind. In July, the zonal moisture fluxes are comparable with the climatology. In contrast, August shows a negative anomaly in zonal moisture flux over the western boundary and almost no anomaly over the eastern boundary. In that month, the western boundary is located in the middle of the high-pressure system, with very low winds, and the eastern boundary is located on the edge of the high-pressure, with higher windspeeds comparable to the climatology.

The meridional flux in May 2003 over the northern boundary is remarkably large. Due to the high pressure over Germany/Poland (Fig. 4c) all moisture is transported northwards over this boundary. The meridional moisture flux over the northern boundary is also in June (7.36) and July (7.97) much larger than the climatology (1.03 and 2.04), indicating much more transport of moisture northwards, and thus out of the Rhine basin. Not more moisture is transported into the basin over the southern boundary in these months, thus resulting in divergence of moisture. In August, we find fluxes of opposite sign, with negative flows of moisture over the northern boundary (thus into the Rhine basin) and south boundary (thus out of the Rhine basin), still leading to divergence of moisture. The southward moisture fluxes are related to the high pressure occurring in August 2003, with northerly winds on the east side of the highest pressure. This anomaly in moisture flux can almost totally be related to an anomaly in the wind compared to the climatology.

Contributions to anomalous moisture fluxes in 2018 In May 2018 we find negative zonal moisture flux over both the eastern and the western boundary, indicating eastern winds. Furthermore, the zonal moisture flux is more negative over the eastern than over the western boundary. The contribution of the anomaly in wind also results in this negative anomaly. In June 2018 we still find slightly eastern winds over the western boundary, while we find slight positive values, thus western wind over the eastern boundary, resulting in large divergence of moisture in this month. From July onwards positive zonal moisture fluxes dominate, although much smaller than the climatology. In August, the zonal moisture fluxes are closest to climatology compared to the rest of the months.

For the meridional moisture fluxes over the northern and southern boundary we find negative values in all months except for the northern boundary in May and August. Thus, instead of the climatological southerlies we have mostly northerlies in 2018, related to the Scandinavian blocking. In August we have the expected southerlies, though double the size as normal. In all months with large anomalies in the moisture flux, we find that this is a result of anomalous wind. In June and July, we find that for both the south and northern boundary the contribution from the multiplied wind and moisture anomaly is opposite in direction of the total anomaly (Fig. 8c and d).

Overall, we can see from the absolute and normalized moisture sources, that the behaviour of the dry summers in 2003 and 2018 are quite different. In 2018, the lack of moisture transport from the Atlantic Ocean and western Europe is very clear, while in 2003 this is not the case, except for August 2003. In May and June 2018, we also find enhanced moisture sources east of the Rhine basin, which are not observed for 2003. Thus, slightly different synoptic situations, with a blocking system located a bit more north or eastwards, can already lead to very different sources, as is found when we compare 2003 and 2018.

Furthermore, we quantified the anomalies in moisture fluxes over the boundaries of the Rhine basin during the summers of 2003 and 2018. We find in both summers anomalous conditions in terms of moisture fluxes, although 2018 is more persistent in the anomalies compared to 2003. In addition, we find that the anomalies in moisture fluxes are mostly related to anomalies in the wind (dynamics). We therefore conclude that the exceptional dynamical situation played an important role in both droughts.
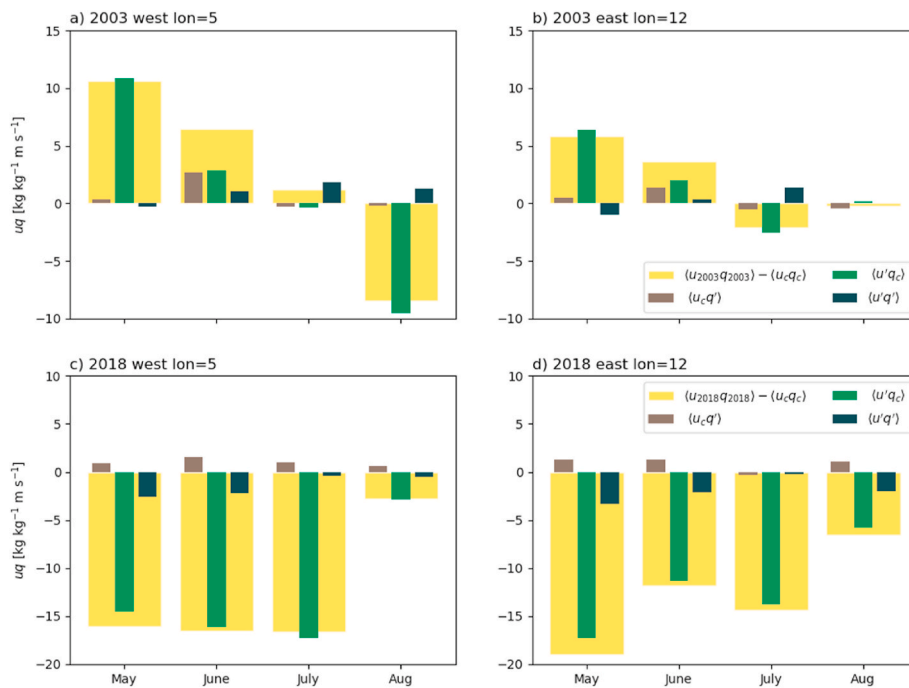
Table 2

Climatological moisture flux $u_c q_c$ and moisture flux occurring in 2003 $u_{2003} q_{2003}$ and 2018 $u_{2018} q_{2018}$ averaged over month and boundary (east and west) in g kg^{-1} m s^{-1}. These are the components of the LHS of Eq (6), when subtracted resulting in the yellow bars in Fig. 7.

	$\langle u_c q_c \rangle$ [g kg^{-1} m s^{-1}]		$\langle u_{2003} q_{2003} \rangle$ [g kg^{-1} m s^{-1}]		$\langle u_{2018} q_{2018} \rangle$ [g kg^{-1} m s^{-1}]	
	west	east	west	east	west	east
May	8.55	6.34	19.19	12.16	−7.53	−12.66
June	16.15	15.04	22.62	18.67	−0.42	3.19
July	21.44	19.54	22.63	17.45	4.84	5.18
August	22.25	18.78	13.76	18.53	19.52	12.25

Table 3

Climatological moisture flux $v_c q_c$ and moisture flux occurring in 2003 $v_{2003} q_{2003}$ and 2018 $v_{2018} q_{2018}$ averaged over month and boundary (north and south) in g kg^{-1} m s^{-1}. These are the components of the LHS of Eq (7), when subtracted resulting in the yellow bars in Fig. 8.

	$\langle v_c q_c \rangle$ [g kg^{-1} m s^{-1}]		$\langle v_{2003} q_{2003} \rangle$ [g kg^{-1} m s^{-1}]		$\langle v_{2018} q_{2018} \rangle$ [g kg^{-1} m s^{-1}]	
	north	south	north	south	north	south
May	3.84	2.68	12.41	4.08	4.93	−0.33
June	1.03	0.74	7.36	1.24	−6.21	−6.17
July	2.04	1.0	7.97	0.52	−3.46	−5.16
August	4.99	2.34	−3.45	−0.93	9.94	−0.33

Fig. 7. Contribution of anomaly in zonal wind $u'\,q_c$, humidity $u_c\,q'$ and both $u'\,q'$ to the monthly anomaly in moisture flux of (a-b) 2003 and (c-d) 2018 compared to the climatology of 1979–2018. Flux contributions are shown for the western (a,c) and eastern boundary (b,d), and all four summer months. Location of the boundaries is shown in Fig. 1.
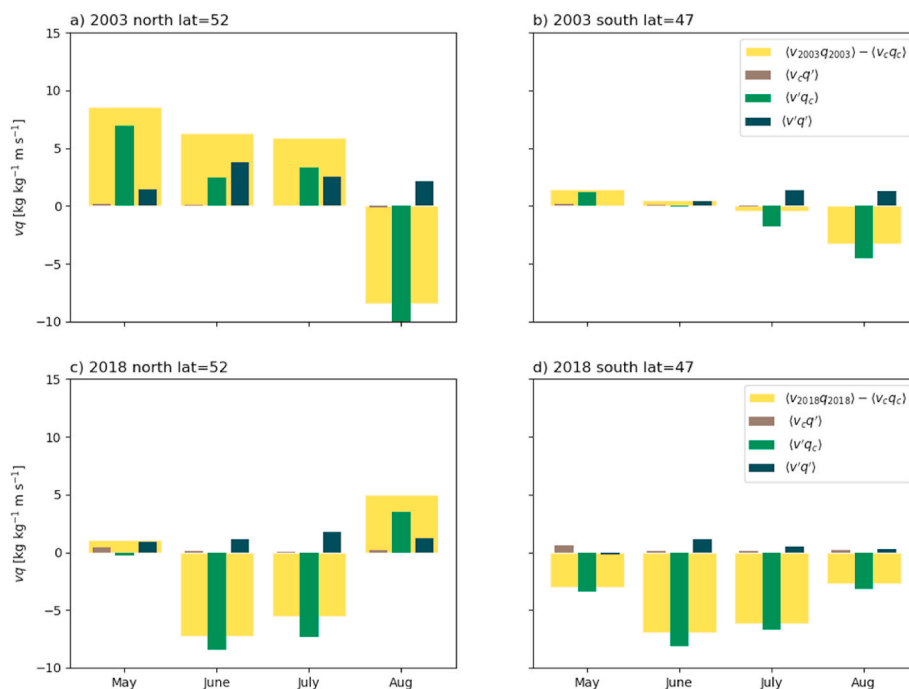

Fig. 8. Contribution of anomaly in meridional wind $v'\,q_c$, humidity $v_c\,q'$ and both $u'\,q'$ to the monthly anomaly in moisture flux of (a–b) 2003 and (c–d) 2018 compared to the climatology of 1979–2018. Flux contributions are shown for the northern (a,c) and southern boundary (b,d), and all four summer months. Location of the boundaries is shown in Fig. 1.

5. Inter-annual variability

Finally, the two driest summers in the Rhine basin of (at least) the last 40 years are put into a longer time perspective by evaluating inter-annual variability in summer precipitation in relation to large-scale synoptics (Section 5.1) and local moisture recycling (Section 5.2).

5.1. Inter-annual variability in Rhine precipitation related to large-scale synoptics

Fig. 9 shows the correlation per grid cell between monthly anomalies of geopotential height at 500 hPa (Z500) and monthly precipitation timeseries over the Rhine basin. The correlation is performed for summer months May, June, July and August for the entire 40-year
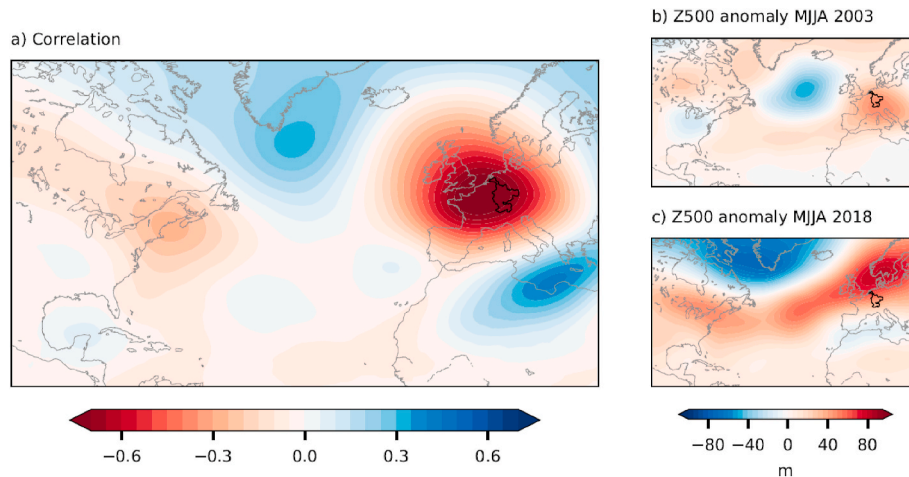
Fig. 9. (a) Spatial correlation of 500 hPa geopotential height anomaly fields (Z500) and precipitation averaged over the Rhine basin. Correlation is performed on 40 years of monthly summer data (May, June, July, August), (b) anomaly of geopotential height at 500 hPa averaged over MJJA 2003 and (c) 2018.

timeseries. Similar results were obtained when the correlation was performed with geopotential height at 850 hPa instead of 500 hPa.

Strong negative correlations are found over western Europe (Fig. 9a), indicating that positive anomalies in Z500 relate to lower-than-normal precipitation values. In other words, high pressure over the Rhine basin relates to dry conditions over this same basin. Values of −0.78 are found just west of the Rhine basin, and are the strongest absolute correlations over the domain, implying that Rhine precipitation is mostly sensitive to its local Z500 value. The negative correlation region is located over the Rhine basin and west of it, indicating that a blocking occurs over the Netherlands, blocking moisture to be transported with the prevailing westerlies from the North Atlantic towards the Rhine basin.

The pattern visible in Fig. 9a clearly resembles the positive phase of the summer North Atlantic Oscillation (NAO), sometimes also called "Blocking" pattern. This summer NAO, is one of the four weather regimes occurring over the North Atlantic during summer (Cassou et al., 2005; Folland et al., 2009), and is associated to dry and warm conditions over western Europe (Cassou et al., 2005; Folland et al., 2009; Lavers et al., 2013; Meehl and Tebaldi, 2004; Pfahl and Wernli, 2012). Furthermore, a persistent anticyclone over the British Isles (as found in Fig. 9a) was associated with a remarkable cooling of the surface waters of the northern North Atlantic (Gervais et al., 2018). Duchez et al. (2016) argues that this negative anomaly in sea surface temperature is the reason for the 2015 heat wave over Europe. Similar negative anomalies in SST were found for 2003 (Black and Sutton, 2007), although not directly related to the heatwave over land. Further investigation is needed to establish the relationship between the North Atlantic cold SSTs, the summer NAO and heat over Europe.

Around western Europe, we find a wave like pattern in the correlation, with positive correlations over southeast Greenland and the Labrador Sea and negative correlations over northeast North America (Fig. 9a). Furthermore, there are positive correlations over the Mediterranean Sea. This 'wave-train' of positive and negative correlations suggest a strongly meandering jet stream (e.g. high amplitude waves). High amplitude waves, with wavenumber 7, are often associated with persistent surface weather conditions, such as dry conditions over western Europe (Kornhuber et al., 2017), together with dry conditions over other parts of the world. This wave-7 pattern occurred throughout the summer of 2018 (mid-June to early July) and at the start of August 2003 (Kornhuber et al., 2019). In addition, Drouard et al. (2019) shows the significant contribution of summer North Atlantic Oscillation by amplifying the wavenumber 7-pattern in extreme summer conditions in Europe from end of June until mid-July 2018. Coumou et al. (2014) provides evidence that many persistent (monthly time scales) weather
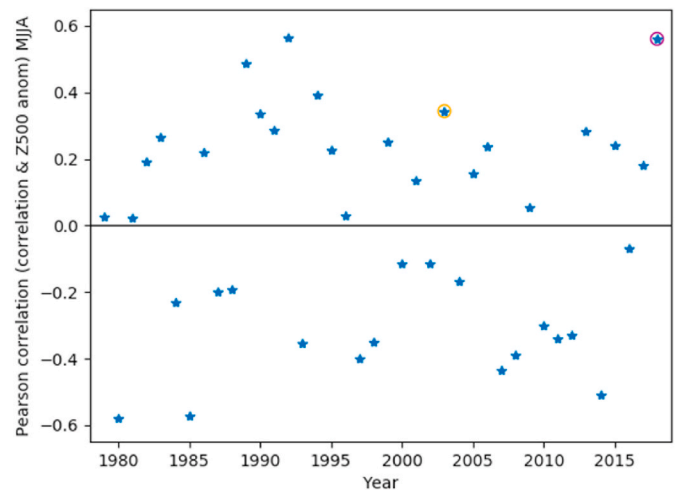

Fig. 10. Pattern correlation of the pattern in Fig. 9a (correlation of precipitation Rhine with Z500 anomaly) with the Z500 anomalies averaged over MJJA per year, with an orange and purple circle for respectively 2003 and 2018. (For interpretation of the references to colour in this figure legend, the reader is referred to the Web version of this article.)

extremes in recent summers were caused by high-amplitude quasi-stationary waves with wave number 6 to 8.

The correlation pattern in Fig. 9a implies the favourable large-scale conditions for dry summers over the Rhine basin, with a strongly meandering jet and blocking located west of the Rhine basin. For comparison, we show the Z500 anomalies during the dry summers 2003 and 2018 (Fig. 9b and c). To further investigate if the large-scale conditions in 2003 and 2018 were indeed very similar to the correlation pattern, and how it compares to other summers we correlate each summer Z500 anomaly with the favourable large-scale conditions for dry summers over the Rhine basin (Fig. 9a). Or differently phrased, is the Z500 anomaly during the 40 years on the location where it reduces the precipitation over the Rhine basin? The results are shown per summer in Fig. 10.

From comparing Fig. 9a and c, we already find that the Z500 anomaly in 2018 is very comparable with the correlation pattern, as is now quantified with a correlation value of 0.6 (Fig. 10). This correlation for 2018 is highest in the 40-year timeseries, indicating the exceptional conditions for a dry summer. In addition, when performing the correlation per month (not shown), all months show a positive correlation,

which did not happen in all other 40 years. Nevertheless, it should be noted that from the Z500 anomaly in 2018 the clear wave-train signal with high amplitude waves is less pronounced. The wave-7 pattern only occurred over two weeks during this summer, and therefore is probably averaged out in this MJJA average. As we have not removed trends here, it might be that we already observe the effect of a northward displacement of the jet in response to climate change (De Vries et al., 2013; Lorenz and DeWeaver, 2007).

The correlation value is positive as well for 2003 (Fig. 10), however not as high as for 2018. The correlations per month show a negative correlation for July 2003, where the other months show clear positive correlations. In addition, we find a clear wave-train (high amplitude wave) in the Z500 anomaly, although the location of the anomalies is shifted compared to the correlation pattern. For 2003 the wave-7 pattern was observed at the start of August (Petoukhov et al., 2013), during the second heatwave of that summer.

Other remarkable years with high correlation values are 1992, 1989 and 1994, but in these years the positive Z500 anomalies were shifted or not as strong and therefore not resulting in dry conditions for the Rhine (Z500 anomalies for 1992, 1989 and 1994 not shown).

5.2. Inter-annual variability in Rhine precipitation related to local moisture recycling

The precipitation recycling ratio is defined in the methodology, and applied to the Rhine basin. It is a common indicator for the amount of moisture recycling within a region. It is the ratio of local precipitation, precipitation related to evaporation which occurred in the basin itself, over total precipitation. Differently formulated; the amount of locally generated precipitation in a region versus the total precipitation (locally generated precipitation and precipitation due to convergence of moisture fluxes by the large-scale flow) in a region. In the summer period this ratio is higher compared to winter, as more evaporation over land takes place in summer, thus the local contribution to precipitation in the Rhine basin is higher. Precipitation recycling indicates the dependence
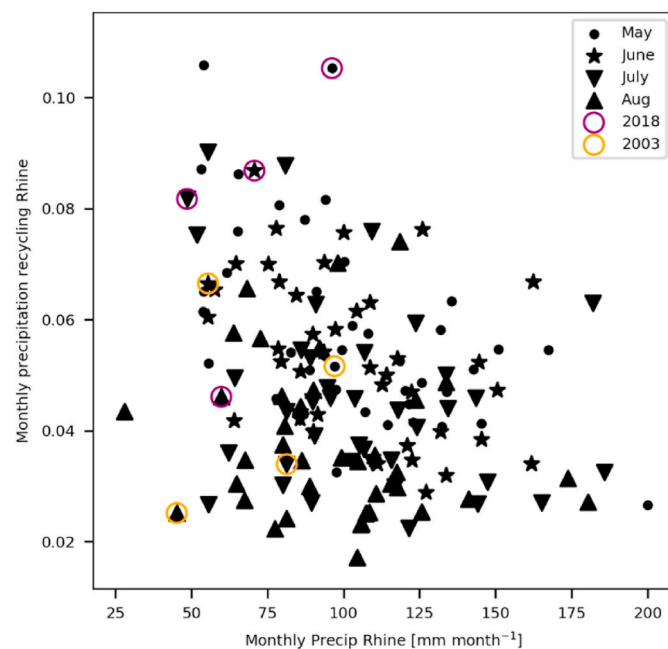

Fig. 11. Scatter plot with monthly precipitation over the Rhine basin in mm month^{-1} against monthly precipitation recycling ratios for the months May, June, July and August, using different symbols to indicate the months. 2003 and 2018 are encircled with respectively orange and purple. (For interpretation of the references to colour in this figure legend, the reader is referred to the Web version of this article.)

of a basin on its local processes, and thus the local land-atmosphere interactions.

In Fig. 11 we show monthly precipitation averaged over the Rhine basin against the monthly precipitation recycling ratio per summer month (May, June, July and August; indicated with different symbols). We find a negative correlation of −0.33, indicating that in dry summer months usually more recycling of moisture takes place compared to wet summer months. This negative relationship between precipitation and precipitation recycling was also found by Bisselink and Dolman (2008), who show for central Europe (including the Rhine basin) that local evaporation contributes more to precipitation in dry summers. Additionally, in the previous section we find a positive correlation of dry summers for the Rhine basin with high pressure over western Europe. And high pressure (e.g. blocking) results in a decrease of moisture advected into the basin, which will lead to an increase in the precipitation recycling ratio. If only the amount of local precipitation decreases, a decrease in precipitation recycling should be observed.

When correlating precipitation and precipitation recycling per month, we find the strongest correlation in May, while it decreases into summer, with lowest correlation in August. Related to this, we find on average higher recycling ratios at the start of summer (0.059 in May and 0.054 in June) and lower recycling ratios at the end of summer (0.046 in July and 0.037 in August). The high ratios in May are related to a relatively small contribution from advection (see Table 2) in this month, while the lower ratios at the end of summer can be related to a general decrease in evaporation, and thus a decrease in precipitation generated by local evaporative fluxes.

In 2003, the recycling ratios in May and June are almost twice as high as in July and August (orange circles in Fig. 11). In June 2003, when the first heatwave occurred, recycling is above average (0.067 in June 2003 compared to 0.054 as climatology). The second heatwave occurred in August 2003, however, the recycling ratio is very low in this particular month (0.025 in 2003 compared to 0.037 in climatology). This indicates that the local precipitation decreased, probably because of dry soils at that point in time, indicating the importance of land-atmosphere feedbacks.

For the summer months in 2018, we find high recycling ratios in combination with low precipitation, especially in May, June and July when the high pressure system was persistent (Fig. 5), and the moisture fluxes did not reach the Rhine catchment (e.g. moisture was not advected into the Rhine basin). In August 2018, precipitation was still low but the advected amount of moisture increased (see Fig. 5k) resulting in a similar precipitation recycling ratio as in the climatology.

It is interesting to see the different characteristics of the recycling ratio in the two dry summers. Much higher recycling ratios are found in May, June and July in 2018 compared to 2003. This indicates the effect of the blocking pattern in 2018, which was more persistent and/or effective in blocking moisture advection into the basin. In addition the strong easterly flow in May and June 2018 contributed to recycling, which did not take place in 2003. Bisselink and Dolman (2009) studied the recycling of moisture over Europe in very wet and dry years, they found that in the dry months June 2003 and July 2006 precipitation recycling is enhanced, which we also found for the Rhine basin (Fig. 11). We conclude that a similar, and stronger, relationship is present for the dry summer of 2018.

Precipitation recycling has been a common approach in the 1990s to study land-atmosphere interactions (Seneviratne et al., 2010), although mainly covering the United States. More specifically, over the Mississippi River basin wet and dry years were studied in terms of moisture recycling, and higher recycling over the Mississippi basin was found during the drought year of 1988 (Bosilovich and Schubert, 2001; Dirmeyer and Brubaker, 1999). Intuitively, it makes sense that more moisture inflow into a region is blocked during dry conditions. As a consequence, it also indicates that a basin during dry conditions depends more on local evaporation, which can decrease substantially during droughts (as in 2003 for the Rhine basin), indicating the importance of
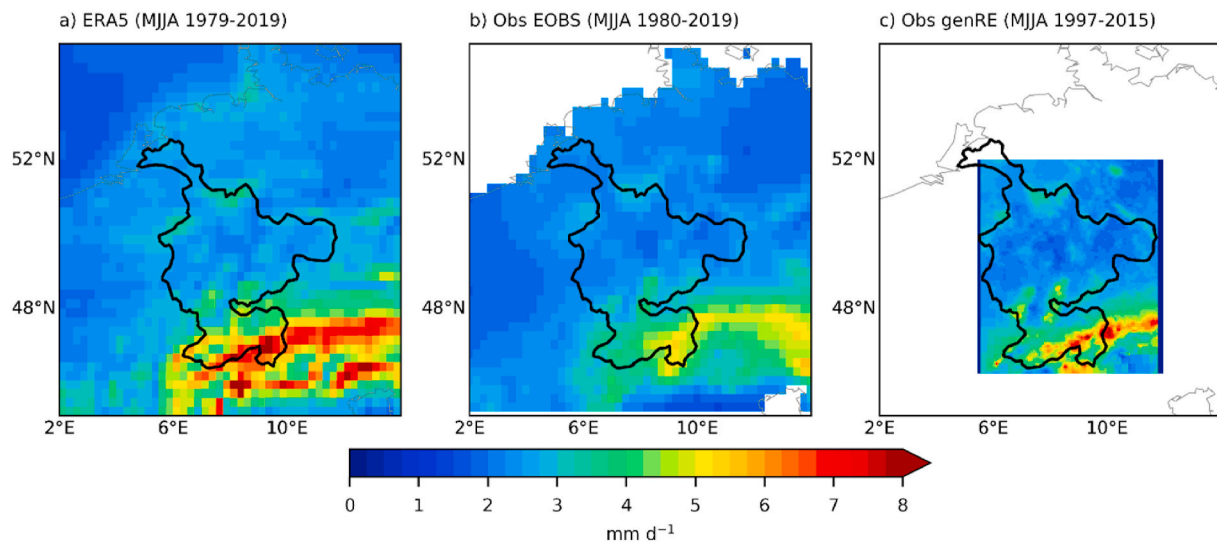
Fig. 12. Daily precipitation sums [mm day^{-1}] averaged over the summer months May, June, July and August (MJJA) over the Rhine basin for (a) ERA5 data from 1979 to 2019, (b) the E-OBS dataset from 1980 to 2019, and (c) the genRE precipitation dataset from 1997 to 2015.

land-atmosphere feedbacks.

6. Discussion on methodology

To determine the moisture sources of the Rhine basin over a long time period, we use the new reanalysis dataset ERA5 and an adapted version of the Eulerian moisture tracking model WAM-2layers. The ERA5 product is state-of-the-art when it comes to data assimilation and high temporal and spatial resolution and provides all needed variables at multiple levels in the atmosphere to perform the tracking. Here, we shortly address the performance of ERA5 to simulate summer convective precipitation over western Europe. Beck et al. (2019) compared ERA5 with the previous reanalysis dataset ERA-Interim across North America, and found ERA5 remarkably better in representing precipitation and land surface variables linked to the terrestrial hydrological cycle (Albergel et al., 2018; Tarek et al., 2020). Fig. 12 shows the daily precipitation amounts averaged over May, June, July and August in ERA5 over western Europe, compared with two observational datasets. The EOBS dataset (Haylock et al., 2008) v21.0e is analysed from 1980 to 2019 with a resolution of 0.25°. The genRE dataset (van Osnabrugge et al., 2017) is available from 1997 up to 2015, with a hourly time resolution, and a spatial resolution of 1.2 km, specifically designed for the Rhine region. We find that in general over the Rhine basin a similar precipitation pattern is found for the ERA5, EOBS and genRE dataset, with higher precipitation amounts over the Alps, but also over the Ardennes, and the black forest in Germany. EOBS seems to underestimate precipitation over the Alps, where less gauge stations are available. This underestimation of precipitation in EOBS in mountainous areas has been reported (Hofstra et al., 2009). From this analysis we can conclude that ERA5 performs well in simulating summer precipitation over the Rhine basin.

We use the Eulerian tracking model WAM-2layers as this model is cost effective, and the adapted version used in this study is validated and shown to perform well for tracking moisture over the Mississippi river basin (Benedict et al., 2019). The largest assumptions in the model are the mixed layer approach, and the vertical transport between the two layers, which is determined from closing the water balance between the two layers (Van der Ent, 2014).

Here, we study the normalized moisture sources of the Rhine basin per month and region. With 6-hourly input data the synoptic patterns are captured and provide enough detail for the monthly average moisture sources. However, when daily sources need to be investigated, a 6-hourly timestep might not be enough. As the tracking is performed on a

limited domain (shown in Fig. 1), moisture sources originating outside of this domain are not accounted for. In addition there is a loss term of water, as the water balance does not close on a daily timescale (Benedict et al., 2019; Findell et al., 2019). Those two factors combined form a residual term, which is 10% on average over MJJA 1979–2018, and 10% and 15% for respectively 2003 and 2018. The larger residual term in 2018 is explained by the anomalous sources from east of the Rhine basin where the domain is relatively limited in extend. The residual term can be higher per individual month as the lifetime of (tracked) moisture in the atmosphere is about 5–10 days (Van der Ent and Tuinenburg, 2017; Läderach and Sodemann, 2016; Trenberth, 1998), and thus moisture related to precipitation in the first days of a month can be accounted for in the preceding month (keep in mind we track moisture backwards in time). This residual term also impacts the precipitation recycling ratio where we assume that all tracked moisture within the Rhine basin in a certain month results in precipitation within that same month.

7. Conclusion and outlook

We studied the similarities and differences in the drought of the summers 2003 and 2018 in terms of Rhine's moisture sources. By analysing moisture sources, evaporative regions which result in precipitation over the Rhine basin, we could study both large-scale processes as local land-atmosphere interactions, and both dynamics and thermodynamics. The combination of different scales (synoptic and local) in view of moisture transport (advection and recycling) provides a new perspective and thereby further insights into the extreme summer droughts of 2003 and 2018.

We determined the moisture sources of the Rhine basin from 1979 to 2018 with a focus on May, June, July and August using ERA5 reanalysis data and an adapted version of the Eulerian moisture tracking model WAM-2layers (Benedict et al., 2019; Van der Ent, 2014). During an average summer, Rhine's moisture sources are mostly located over the Atlantic Ocean, together with a large contribution from continental evaporation, mostly from regions west of the Rhine basin (Fig. 6).

The droughts of 2003 and 2018 stand out as the driest summers in the 40-year timeseries in terms of precipitation over the Rhine basin. Both are two standard deviations below the mean precipitation over May, June, July and August. In both summers we find a decrease in absolute moisture sources from oceanic regions, although the normalized contributions are different between the two years (Fig. 6). The anomalous moisture fluxes over the boundaries of the Rhine basin in 2003 and 2018 are a result of anomalies in wind, thus anomalous

dynamics (Figs. 7 and 8). The differences in normalized sources are due to the different locations and persistence of the high-pressure systems, blocking moisture to be transported to the Rhine basin. We find that 2018 is most favourable in terms of large-scale synoptics to result in dry conditions over the Rhine basin, while this is to a lesser extent the case for 2003 (Figs. 9 and 10). When focusing on land-atmosphere interactions, we found in general higher recycling of moisture within the basin under drier conditions. This relationship was observed for 2018, as a decrease in moisture advected into the basin resulted in higher recycling. In August 2003 however, recycling was lower than normal, although it was very dry, indicating a smaller contribution of local precipitation in this month probably due to drying out of the soils, which enhanced the heatwave (Fischer et al., 2007).

Here, we have analysed two past drought events in terms of moisture sources. Using this methodology, there is also potential to study droughts in seasonal prediction, as is currently relevant seeing the dry conditions for Western Europe in the spring of 2020, and under future projections, for example to indicate vulnerability to land-use changes. By studying moisture sources and recycling during droughts, we capture both the large-scale circulation and land-atmosphere interactions. To further enhance our understanding on these processes we need case specific studies, as by analysing composites and statistics, important processes playing a role cannot be distinguished. This study highlights the unique nature of the two droughts of 2003 and 2018 that we studied.

Author statement

All authors contributed to the idea and design of this work. IB performed the experiments, the data analysis, and wrote the manuscript. All authors commented on the manuscript.

Declaration of competing interest

The authors declare that they have no known competing financial interests or personal relationships that could have appeared to influence the work reported in this paper.

Acknowledgments

References

Albergel, C., Dutra, E., Munier, S., Calvet, J.-C., Munoz-Sabater, J., Rosnay, P., de Balsamo, G., 2018. ERA-5 and ERA-Interim driven ISBA land surface model simulations: which one performs better? Hydrol. Earth Syst. Sci. 22, 3515–3532. https://doi.org/10.5194/hess-22-3515-2018.

Benedict, I., van Heerwaarden, C.C., van der Ent, R.J., Weerts, A.H., Hazeleger, W., 2019. Decline in terrestrial moisture sources of the Mississippi river basin in a future climate. J. Hydrometeorol. 21, 299–316. https://doi.org/10.1175/JHM-D-19-0094.1.

Beniston, M., 2004. The 2003 heat wave in Europe: a shape of things to come? An analysis based on Swiss climatological data and model simulations. Geophys. Res. Lett. 31 https://doi.org/10.1029/2003GL018857.

Bisselink, B., Dolman, A.J., 2009. Recycling of moisture in Europe: contribution of evaporation to variability in very wet and dry years. Hydrol. Earth Syst. Sci. 13, 1685–1697. https://doi.org/10.5194/hess-13-1685-2009.

Bisselink, B., Dolman, A.J., 2008. Precipitation recycling: moisture sources over Europe using ERA-40 data. J. Hydrometeorol. 9, 1073–1083. https://doi.org/10.1175/2008JHM962.1.

Black, E., Blackburn, M., Harrison, G., Hoskins, B., Methven, J., 2004. Factors contributing to the summer 2003 European heatwave. Weather 59, 217–223. https://doi.org/10.1256/wea.74.04.

Black, E., Sutton, R., 2007. The influence of oceanic conditions on the hot European summer of 2003. Clim. Dynam. 28, 53–66. https://doi.org/10.1007/s00382-006-0179-8.

Bosilovich, M.G., Schubert, S.D., 2001. Precipitation recycling over the Central United States diagnosed from the GEOS-1 data assimilation system. J. Hydrometeorol. 2, 26–35. https://doi.org/10.1175/1525-7541(2001)002<0026:PROTCU>2.0.CO;2.

Brubaker, K.L., Dirmeyer, P.A., Sudradjat, A., Levy, B.S., Bernal, F., 2001. A 36-yr climatological description of the evaporative sources of warm-season precipitation in the Mississippi river basin. J. Hydrometeorol. 2, 537–557. https://doi.org/10.1175/1525-7541(2001)002<0537:AYCDOT>2.0.CO;2.

Cassou, C., Terray, L., Phillips, A.S., 2005. Tropical atlantic influence on European heat waves. J. Clim. 18, 2805–2811. https://doi.org/10.1175/JCLI3506.1.

Coumou, D., Petoukhov, V., Rahmstorf, S., Petri, S., Schellnhuber, H.J., 2014. Quasi-resonant circulation regimes and hemispheric synchronization of extreme weather in boreal summer. Proc. Natl. Acad. Sci. Unit. States Am. 111, 12331–12336. https://doi.org/10.1073/pnas.1412797111.

De Vries, H., Woollings, T., Anstey, J., Haarsma, R.J., Hazeleger, W., 2013. Atmospheric blocking and its relation to jet changes in a future climate. Clim. Dynam. 41, 2643–2654. https://doi.org/10.1007/s00382-013-1699-7.

Dirmeyer, P.A., Brubaker, K.L., 1999. Contrasting evaporative moisture sources during the drought of 1988 and the flood of 1993. J. Geophys. Res. Atmospheres 104, 19383–19397. https://doi.org/10.1029/1999JD900222.

Dominguez, F., Kumar, P., Liang, X.-Z., Ting, M., 2006. Impact of atmospheric moisture storage on precipitation recycling. J. Clim. 19, 1513–1530. https://doi.org/10.1175/JCLI3691.1.

Drouard, M., Kornhuber, K., Woollings, T., 2019. Disentangling dynamic contributions to summer 2018 anomalous weather over Europe. Geophys. Res. Lett. 46, 12537–12546. https://doi.org/10.1029/2019GL084601.

Duchez, A., Frajka-Williams, E., Josey, S.A., Evans, D.G., Grist, J.P., Marsh, R., McCarthy, G.D., Sinha, B., Berry, D.I., Hirschi, J.J.-M., 2016. Drivers of exceptionally cold North Atlantic Ocean temperatures and their link to the 2015 European heat wave. Environ. Res. Lett. 11, 074004 https://doi.org/10.1088/1748-9326/11/7/074004.

Ferranti, L., Viterbo, P., 2006. The European summer of 2003: sensitivity to soil water initial conditions. J. Clim. 19, 3659–3680. https://doi.org/10.1175/JCLI3810.1.

Findell, K.L., Keys, P.W., van der Ent, R.J., Lintner, B.R., Berg, A., Krasting, J.P., 2019. Rising temperatures increase importance of oceanic evaporation as a source for continental precipitation. J. Clim. 32 (33), 7713–7726.

Fischer, E.M., Seneviratne, S.I., Vidale, P.L., Lüthi, D., Schär, C., 2007. Soil moisture–atmosphere interactions during the 2003 European summer heat wave. J. Clim. 20, 5081–5099. https://doi.org/10.1175/JCLI4288.1.

Folland, C.K., Knight, J., Linderholm, H.W., Fereday, D., Ineson, S., Hurrell, J.W., 2009. The summer North atlantic oscillation: past, present, and future. J. Clim. 22, 1082–1103. https://doi.org/10.1175/2008JCLI2459.1.

Gervais, M., Shaman, J., Kushnir, Y., 2018. Mechanisms governing the development of the north atlantic warming hole in the CESM-LE future climate simulations. J. Clim. 31, 5927–5946. https://doi.org/10.1175/JCLI-D-17-0635.1.

Haylock, M.R., Hofstra, N., Klein Tank, A.M.G., Klok, E.J., Jones, P.D., New, M., 2008. A European daily high-resolution gridded data set of surface temperature and precipitation for 1950–2006. J. Geophys. Res. 113 https://doi.org/10.1029/2008JD010201.

Hazeleger, W., van den Hurk, B.J.J.M., Min, E., van Oldenborgh, G.J., Petersen, A.C., Stainforth, D.A., Vasileiadou, E., Smith, L.A., 2015. Tales of future weather. Nat. Clim. Change 5, 107–113. https://doi.org/10.1038/nclimate2450.

Herrera-Estrada, J.E., Martinez, J.A., Dominguez, F., Findell, K.L., Wood, E.F., Sheffield, J., 2019. Reduced moisture transport linked to drought propagation across North America. Geophys. Res. Lett. 46, 5243–5253.

Hersbach, H., Bell, B., Berrisford, P., Hirahara, S., Horányi, A., Muñoz-Sabater, J., Nicolas, J., Peubey, C., Radu, R., Schepers, D., Simmons, A., Soci, C., Abdalla, S., Abellan, X., Balsamo, G., Bechtold, P., Biavati, G., Bidlot, J., Bonavita, M., Chiara, G. D., Dahlgren, P., Dee, D., Diamantakis, M., Dragani, R., Flemming, J., Forbes, R., Fuentes, M., Geer, A., Haimberger, L., Healy, S., Hogan, R.J., Hólm, E., Janisková, M., Keeley, S., Laloyaux, P., Lopez, P., Lupu, C., Radnoti, G., de Rosnay, P., Rozum, I., Vamborg, F., Villaume, S., Thépaut, J.-N., 2020. The ERA5 global reanalysis. Q. J. R. Meteorol. Soc. 146 (730), 1999–2049. https://doi.org/10.1002/qj.3803.

Hofstra, N., Haylock, M., New, M., Jones, P.D., 2009. Testing E-OBS European high-resolution gridded data set of daily precipitation and surface temperature. J. Geophys. Res. 114 https://doi.org/10.1029/2009JD011799.

Kornhuber, K., Osprey, S., Coumou, D., Petri, S., Petoukhov, V., Rahmstorf, S., Gray, L., 2019. Extreme weather events in early summer 2018 connected by a recurrent hemispheric wave-7 pattern. Environ. Res. Lett. 14, 054002 https://doi.org/10.1088/1748-9326/ab13bf.

Kornhuber, K., Petoukhov, V., Karoly, D., Petri, S., Rahmstorf, S., Coumou, D., 2017. Summertime planetary wave resonance in the northern and southern hemispheres. J. Clim. 30, 6133–6150. https://doi.org/10.1175/JCLI-D-16-0703.1.

Läderach, A., Sodemann, H., 2016. A revised picture of the atmospheric moisture residence time. Geophys. Res. Lett. 43, 924–933. https://doi.org/10.1002/2015GL067449.

Lavers, D., Prudhomme, C., Hannah, D.M., 2013. European precipitation connections with large-scale mean sea-level pressure (MSLP) fields. Hydrol. Sci. J. 58, 310–327. https://doi.org/10.1080/02626667.2012.754545.

Lorenz, D.J., DeWeaver, E.T., 2007. Tropopause height and zonal wind response to global warming in the IPCC scenario integrations. J. Geophys. Res. Atmospheres 112. https://doi.org/10.1029/2006JD008087.

Meehl, G.A., Tebaldi, C., 2004. More intense, more frequent, and longer lasting heat waves in the 21st century. Science 305, 994–997. https://doi.org/10.1126/science.1098704.

Miralles, D.G., Gentine, P., Seneviratne, S.I., Teuling, A.J., 2019. Land–atmospheric feedbacks during droughts and heatwaves: state of the science and current challenges. Ann. N. Y. Acad. Sci. 1436, 19–35. https://doi.org/10.1111/nyas.13912.

Petoukhov, V., Rahmstorf, S., Petri, S., Schellnhuber, H.J., 2013. Quasiresonant amplification of planetary waves and recent Northern Hemisphere weather extremes. Proc. Natl. Acad. Sci. Unit. States Am. 110, 5336–5341. https://doi.org/10.1073/pnas.1222000110.

Pfahl, S., Wernli, H., 2012. Quantifying the relevance of atmospheric blocking for co-located temperature extremes in the Northern Hemisphere on (sub-)daily time scales. Geophys. Res. Lett. 39 https://doi.org/10.1029/2012GL052261.

Philip, S.Y., Kew, S.F., van der Wiel, K., Wanders, N., van Oldenborgh, G.J., 2020. Regional differentiation in climate change induced drought trends in The Netherlands. Environ. Res. Lett. 15, 094081 https://doi.org/10.1088/1748-9326/ab97ca.

Rosner, B., Benedict, I., Van Heerwaarden, C., Weerts, A., Hazeleger, W., Bissoli, P., Trachte, K., 2019. Sidebar 7.3: the long heat wave and drought in Europe in 2018, 9. In: State of the Climate in 2018, vol. 100. Bull. Amer. Meteor. Soc.. S222–S223.

Roy, T., Martinez, J.A., Herrera-Estrada, J.E., Zhang, Y., Dominguez, F., Berg, A., Ek, M., Wood, E.F., 2018. Role of moisture transport and recycling in characterizing droughts: perspectives from two recent U.S. Droughts and the CFSv2 system. J. Hydrometeorol. 20, 139–154. https://doi.org/10.1175/JHM-D-18-0159.1.

Schär, C., Jendritzky, G., 2004. Hot news from summer 2003. Nature 432, 559–560. https://doi.org/10.1038/432559a.

Schär, C., Vidale, P.L., Lüthi, D., Frei, C., Häberli, C., Liniger, M.A., Appenzeller, C., 2004. The role of increasing temperature variability in European summer heatwaves. Nature 427, 332–336. https://doi.org/10.1038/nature02300.

Schiemann, R., Demory, M.-E., Shaffrey, L.C., Strachan, J., Vidale, P.L., Mizielinski, M.S., Roberts, M.J., Matsueda, M., Wehner, M.F., Jung, T., 2016. The resolution sensitivity of northern Hemisphere blocking in four 25-km atmospheric global circulation models. J. Clim. 30, 337–358. https://doi.org/10.1175/JCLI-D-16-0100.1.

Seneviratne, S.I., Corti, T., Davin, E.L., Hirschi, M., Jaeger, E.B., Lehner, I., Orlowsky, B., Teuling, A.J., 2010. Investigating soil moisture–climate interactions in a changing climate: a review. Earth Sci. Rev. 99, 125–161. https://doi.org/10.1016/j.earscirev.2010.02.004.

Shepherd, T.G., 2016. A common framework for approaches to extreme event attribution. Curr. Clim. Change Rep. 2, 28–38. https://doi.org/10.1007/s40641-016-0033-y.

Shepherd, T.G., 2014. Atmospheric circulation as a source of uncertainty in climate change projections. Nat. Geosci. 7, 703–708. https://doi.org/10.1038/ngeo2253.

Spensberger, C., Madonna, E., Boettcher, M., Grams, C.M., Papritz, L., Quinting, J.F., Röthlisberger, M., Sprenger, M., Zschenderlein, P., 2020. Dynamics of concurrent and sequential Central European and Scandinavian heatwaves. Q. J. R. Meteorol. Soc. 146 (732), 2998–3013. https://doi.org/10.1002/qj.3822.

Stojanovic, M., Drumond, A., Nieto, R., Gimeno, L., 2018. Anomalies in moisture supply during the 2003 drought event in Europe: a Lagrangian analysis. Water 10, 467. https://doi.org/10.3390/w10040467.

Stott, P.A., Stone, D.A., Allen, M.R., 2004. Human contribution to the European heatwave of 2003. Nature 432, 610–614. https://doi.org/10.1038/nature03089.

Tarek, M., Brissette, F.P., Arsenault, R., 2020. Evaluation of the ERA5 reanalysis as a potential reference dataset for hydrological modelling over North America. Hydrol. Earth Syst. Sci. 24, 2527–2544. https://doi.org/10.5194/hess-24-2527-2020.

Toreti, A., Belward, A., Perez-Dominguez, I., Naumann, G., Luterbacher, J., Cronie, O., Seguini, L., Manfron, G., Lopez-Lozano, R., Baruth, B., van den Berg, M., Dentener, F., Ceglar, A., Chatzopoulos, T., Zampieri, M., 2019. The exceptional 2018 European water seesaw calls for action on adaptation. Earths Future 7, 652–663. https://doi.org/10.1029/2019EF001170.

Trenberth, K.E., 1998. Atmospheric moisture residence times and cycling: implications for rainfall rates and climate change. Climatic Change 39, 667–694. https://doi.org/10.1023/A:1005319109110.

Van der Ent, R.J., 2014. A new view on the hydrological cycle over continents. PhD Thesis.

Van der Ent, R.J., Tuinenburg, O.A., 2017. The residence time of water in the atmosphere revisited. Hydrol. Earth Syst. Sci. 21, 779–790. https://doi.org/10.5194/hess-21-779-2017.

van der Ent, R.J., Tuinenburg, O.A., Knoche, H.-R., Kunstmann, H., Savenije, H.H.G., 2013. Should we use a simple or complex model for moisture recycling and atmospheric moisture tracking? Hydrol. Earth Syst. Sci. 17, 4869–4884. https://doi.org/10.5194/hess-17-4869-2013.

Van der Ent, R.J., Wang-Erlandsson, L., Keys, P.W., Savenije, H.H.G., 2014. Contrasting roles of interception and transpiration in the hydrological cycle – Part 2. Moisture recycling. Earth Syst. Dyn 5, 471–489. https://doi.org/10.5194/esd-5-471-2014.

Van der Ent, Rudi J., Savenije, H.H.G., Schaefli, B., Steele-Dunne, S.C., 2010. Origin and fate of atmospheric moisture over continents. Water Resour. Res. 46 https://doi.org/10.1029/2010WR009127.

van Osnabrugge, B., Weerts, A., Uijlenhoet, R., 2017. genRE: A Method to Extend Gridded Precipitation Climatology Data Sets in Near Real-Time for Hydrological Forecasting Purposes. https://doi.org/10.1002/2017WR021201. Water Resour. Res.

Vogel, M.M., Zscheischler, J., Wartenburger, R., Dee, D., Seneviratne, S.I., 2019. Concurrent 2018 hot extremes across northern Hemisphere due to human-induced climate change. Earths Future 7, 692–703. https://doi.org/10.1029/2019EF001189.

Wehrli, K., Hauser, M., Seneviratne, S.I., 2020. Storylines of the 2018 Northern Hemisphere Heat Wave at Pre-industrial and Higher Global Warming Levels (Preprint). https://doi.org/10.5194/esd-2019-91. Earth system change: climate scenarios.

Woollings, T., 2010. Dynamical influences on European climate: an uncertain future. Philos. Trans. R. Soc. Math. Phys. Eng. Sci. 368, 3733–3756. https://doi.org/10.1098/rsta.2010.0040.

Zangvil, A., Portis, D.H., Lamb, P.J., 2004. Investigation of the large-scale Atmospheric moisture field over the midwestern United States in relation to summer precipitation. Part II: recycling of local evapotranspiration and association with soil moisture and crop yields. J. Clim. 17, 3283–3301. https://doi.org/10.1175/1520-0442(2004)017<3283:IOTLAM>2.0.CO;2.

Zangvil, A., Portis, D.H., Lamb, P.J., 2001. Investigation of the large-scale Atmospheric moisture field over the midwestern United States in relation to summer precipitation. Part I: relationships between moisture budget components on different timescales. J. Clim. 14, 582–597. https://doi.org/10.1175/1520-0442(2001)014<0582:IOTLSA>2.0.CO;2.